LARGE-SCALE GAS DYNAMICAL PROCESSES AFFECTING THE ORIGIN AND EVOLUTION OF GASEOUS GALACTIC HALOS

PAUL R. SHAPIRO
Department of Astronomy
The University of Texas at Austin
Austin, Texas 78712, U.S.A.

ABSTRACT. Observations of galactic halo gas are consistent with an interpretation in terms of the galactic fountain model in which supernova heated gas in the galactic disk escapes into the halo, radiatively cools and forms clouds which fall back to the disk. The results of a new study of several large-scale gas dynamical effects which are expected to occur in such a model for the origin and evolution of galactic halo gas will be summarized, including the following: (1) nonequilibrium absorption line and emission spectrum diagnostics for radiatively cooling halo gas in our own galaxy, as well the implications of such absorption line diagnostics for the origin of quasar absorption lines in galactic halo clouds of high redshift galaxies; (2) numerical MHD simulations and analytical analysis of large-scale explosions and superbubbles in the galactic disk and halo; (3) numerical MHD simulations of halo cloud formation by thermal instability, with and without magnetic field; and (4) the effect of the galactic fountain on the galactic dynamo.

1. INTRODUCTION

In what follows, I summarize the results of several new theoretical investigations whose common goal is the elucidation of the origin and nature of galactic halo gas. This work, it is hoped, will "flesh out" some of the expectations and implications of the galactic fountain model of Shapiro and Field (1976) in order to determine how well it explains the observed properties of interstellar disk and halo gas and their interaction. The reader is referred to Spitzer (1990) for a recent review of and references to other work in this field.

2. NONEQUILIBRIUM ABSORPTION LINE AND EMISSION SPECTRUM DIAGNOSTICS FOR RADIATIVELY COOLING GALACTIC HALO GAS

Observations of ultraviolet absorption and emission lines in interstellar gas at large distance from the galactic plane have been interpreted in terms of a gaseous galactic halo in which hot gas ($\sim 10^6$ K) is radiatively cooling and recombining as in the galactic fountain model. As the first step in a new investigation of the observable properties of such halo gas, we have recalculated the nonequilibrium radiative cooling, ionization, and recombination of an optically thin gas composed of the 13 elements H, He, C, N, O, Ne, Na, Mg, Si, S, Ca, Fe, and Ni (Shapiro and Benjamin 1990). We use the abundances of Allen (1973) and the atomic data of Raymond and Smith (1977) and Raymond (1987). We have solved the ionization balance rate equations together with the equation of energy

H. Bloemen (ed.), The Interstellar Disk-Halo Connection in Galaxies, 417–428.

conservation for a gas cooling from 10^6 K to 10^4 K at either constant density (isochoric) or constant pressure (isobaric), including the effects of photoionization by an ambient radiation field contributed by galactic stars and supernova remnants and the metagalactic radiation background. These limiting isochoric and isobaric cases correspond, respectively, to the cases where the cooling regions are large enough for the sound crossing time to exceed the cooling time or vice versa. The UV absorption line spectrum as well as the emergent line and continuum spectrum in the soft X-ray and UV wavelengths have been calculated and compared with current observations. We have also considered other types of incident radiation and applied our results to the question of the origin of quasar absorption lines in galactic halo clouds.

2.1 The Galactic Fountain and Milky Way Halo Gas

We assume a steady-state, plane-parallel, optically thin flow of halo gas out of the galactic disk, with initial velocity v_0 and initial total hydrogen density $n_{H,0}$. The outflowing gas starts in ionization equilibrium at a temperature of 10^6 K. Column densities through the flow for an ionic species i are given by $n_{H,0}v_0\int dty_i = N_H(t)\langle y_i\rangle_t$, where $y_i = n_i/n_H$, time t is measured from the initial time at which the fluid element is at 10^6 K, $N_H(t)$ is the total H column density between the base of the flow and the position of the fluid element at time t, and $\langle y_i\rangle_t$ is the time-average of y_i between t = 0 and t. For cases without photoionization included, the product $N_H(t)\langle y_i\rangle_t$ reaches an asymptotic value for times greater than a few initial cooling times. For cases with photoionization, however, the gas relaxes to thermal and ionization equilibrium, and the column densities of some ions (e.g. C IV and Si IV in the isobaric case, and all ions shown here in the isochoric case), thereafter, grow in proportion to time for t greater than this relaxation time.

A selection of our results for the column densities of C IV, N V and Si IV and the temperature versus total H column density is presented in Figures 1(a) and (b), along with the observed column density ratios for Milky Way halo gas from Savage and Massa (1987), as summarized by Savage (1988). For cases which include an incident ionizing radiation field, we adopt the spectrum of Bregman and Harrington (1986) and vary the flux level by adjusting the ionization parameter $\Gamma = n_\gamma/n_{H,0}$, where n_γ is the number density of H ionizing photons in the incident radiation field. There is a convenient scaling property for these results such that, for a fixed spectral shape and value of Γ, the results for different values of v_o and $n_{H,0}$ are the same if plotted versus $N_H(t)/v_o = n_{H,0}t$. The mass circulation rate for the entire galaxy in $M_\odot$ per year implied by the steady presence of the corresponding particle flux $n_{H,0}$ v_o over a fraction f of the galactic disk of area πR^2 with R = 15 kpc is $\dot{M} \approx 2.5\ (n_{H,0}/10^{-3}\ cm^{-3})(v_o/100\ km\ s^{-1})f$. Our results *without* photoionization agree reasonably well with those of Edgar and Chevalier (1986), although we have included charge exchange reactions while their calculations did not. We find that, for $\Gamma = 0$, the asymptotic values of N(C IV)/v_o are $\approx 10^7$ cm^{-3} s and $10^{6.3}$ cm^{-3} s for the isochoric and isobaric limits, respectively, implying that the observed value N(C IV) $\approx$ 10^{14} cm^{-2} requires $v_o \sim 100$ km s^{-1} and $v_o \sim 600$ km s^{-1} for each of these cases. The former value of v_o is consistent with the expectations of a galactic fountain flow, while the latter is a bit too high to be reasonable. In addition, neither case reproduces the observed ratios.

With photoionization, the isochoric limit succeeds in reproducing the observed column density ratios at the same point that it achieves N(C IV) $\approx 10^{14}$ cm^{-2} as long as the flux level is in the range $10^{-1.8} \lesssim \Gamma \lesssim 10^{-2.7}$ and $v_o \sim 100$ km s^{-1}. The isobaric limit, however, fails again even for very large flux levels. This suggests that the cooling regions are initially large enough [i.e. size $\gtrsim$ 1 kpc $(n_{H,0}/10^{-2}\ cm^{-3})^{-1}$] that an isochoric

https://doi.org/10.1017/S0074180900089373 Published online by Cambridge University Press

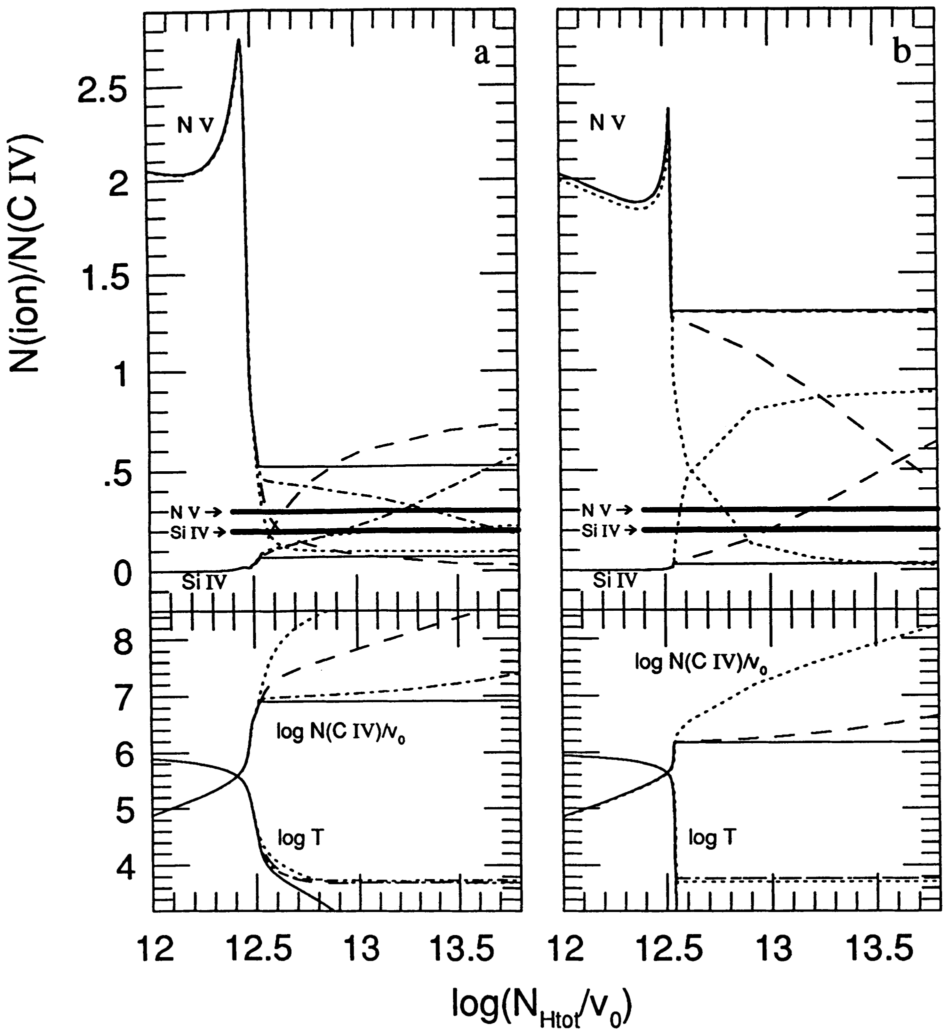

Figure 1. (a) (Upper panel) Column density ratios N(N V)/N(C IV) (descending curves) and N(Si IV)/N(C IV) (ascending curves) versus N(H)/v_0 for isochoric cases with no photoionization (solid line), and with an external photoionization field with log $\Gamma = -1.2$ (dotted), log $\Gamma = -2.2$ (dashed), and log $\Gamma = -3.1$ (dash-dot). The observed column density ratios are indicated with bold lines. (Lower panel) Temperature and N(C IV)/v_0 versus N(H)/v_0. (b) Same as (a), but with isobaric cooling, for cases with no photoionization (solid line), and an external photoionization field with log $\Gamma = -0.2$ (dotted), log $\Gamma = -1.2$ (dashed), and log $\Gamma = -2.2$ (dash-dot).

description is more appropriate than an isobaric one. The required flux level range given above can be compared with previous estimates of the ambient ionizing flux level to which halo gas is exposed. Bregman and Harrington (1986) estimated $\Gamma = \Gamma_{BH} = 10^{-1.2}$ $(n_{H,0}/10^{-3}\ cm^{-3})^{-1}$, implying $3\times10^{-2} \gtrsim n_{H,0} \gtrsim 3\times10^{-3}\ cm^{-3}$ in order to make $\Gamma_{required} = \Gamma_{BH}$. Recently, more restrictive limits have been claimed for Γ, based upon attempts to detect $H\alpha$ recombination emission from halo clouds. Kutyrev and Reynolds (1989) claim $\Gamma \lesssim \Gamma_{KR} = 10^{-2.2}\ (n_{H,0}/10^{-3}\ cm^{-3})^{-1}$, while Songaila, Bryant, and Cowie (1989) claim $\Gamma \lesssim \Gamma_{SBC} = 10^{-2.7}\ (n_{H,0}/10^{-3}\ cm^{-3})^{-1}$. In that case, $n_{H,0} \sim 10^{-3}\ cm^{-3}$ makes our results consistent with these limits.

We have also calculated the emergent radiation spectrum of the cooling fountain flow. For external $\Gamma = 0$, a convenient scaling property exists such that the quantity $\phi_\nu = I_\nu/(n_{H,0}v_0)$ is constant with respect to variations of $n_{H,0}$ and v_0, where I_ν is the emergent intensity at frequency ν. Martin and Bowyer (1990) recently reported the detection of UV emission lines of C IV and O III from the galactic halo. We find that, in order to match the observed intensity of these lines while at the same time satisfying the absorption-line data as described above, $n_{H,0} \approx 2\times10^{-2}\ cm^{-2}$ and $v_0 \sim 100\ km\ s^{-1}$ are required for the isochoric case. This density makes the external photoionizing flux level required to reproduce the C IV, Si IV, and N V absorption-line data exceed the limit suggested, for example, by Kutyrev and Reynolds (1989) by a factor of several. However, such limits are subject to reinterpretation if the neutral halo gas which was observed in $H\alpha$ emission was actually exposed to an attenuated or diluted version of the flux which ionizes the gas in the fountain flow.

A remarkable new result which emerges from these calculations is that the ionizing radiation emitted by the cooling fountain flow itself is sufficient to photoionize the flow so as to reproduce the observed column densities of C IV, Si IV, and N V. The flux level of this self-ionization spectrum corresponds to $\Gamma_{self} = (v_0/c)\phi$, where $\phi = \int(\phi_\nu/h\nu)d\nu$ from $\nu = 13.6$ eV/h to $\nu = \infty$. We find $\phi \approx 3.7$ for the isochoric case, and, hence, $\Gamma_{self} \cong 10^{-2.9}$ $(v_0/100\ km\ s^{-1})$. The observed line ratios are matched for $v_0 \sim 100\ km\ s^{-1}$. This Γ_{self} is somewhat less than that required if the photoionization is attributed instead to external sources, so the self-ionization spectrum is more efficient at photoionizing the flow. In short, a cooling fountain flow can explain both the observed UV absorption and emission lines of galactic halo gas by absorbing its own photoionizing emission as it cools, if $n_{H,0} \sim 2\times10^{-2}\ cm^{-3}$, $v_0 \sim 100\ km\ s^{-1}$, and the initial size of the cooling region is several hundreds of parsecs or more.

2.2 The Galactic Fountain and Quasar Absorption Lines

Can the same cooling fountain flow explain the observed quasar absorption lines of Lyman limit systems at $z \sim 3$? We have plotted in Figure 2 a selection of our results for the column densities of C II, C III, Si III, and Si IV relative to that of C IV, versus N(H I)/v_0, for the same isochoric, steady-state cooling flow as described above in § 2.1. We have also plotted the observed values for a cloud with N(H I) $\cong 10^{17.5}\ cm^{-2}$ at $z_{abs} = 2.9676$ in the spectrum of PKS 2126–158 ($z_{em} = 3.27$) reported by Sargent, Steidel, and Boksenberg (1990). The relative metal abundances are from Allen (1973) as before, but the overall metal abundance relative to H is adjusted in order to match the observed ratio N(C IV)/N(H I). In Figure 2(a), the incident ionizing spectrum is that for gas in our own galactic halo estimated by Bregman and Harrington (1986), while that in Figure 2(b) was a metagalactic ionizing background at $z \sim 3$ calculated by Giroux and Shapiro (1990) for AGN-type sources distributed throughout a cosmologically evolving intergalactic medium.

We find that, without the effects of photoionization included, cooling fountain gas does not match the data. With photoionization, however, a fountain flow *can* explain the data.

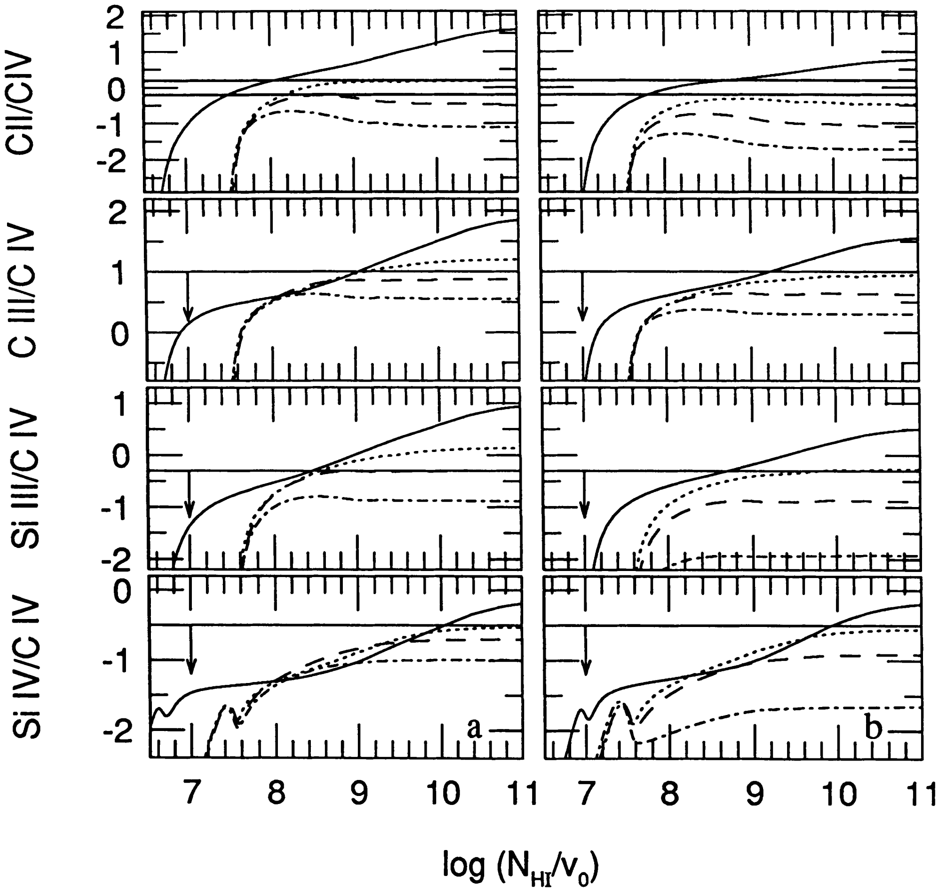

Figure 2. (a) Log (N(ion)/N(C IV)) for isochorically cooling gas with a galaxy type spectrum from Bregman and Harrington (1986), with log Γ –2.7 (solid), log $\Gamma = -2.0$ (dotted), log $\Gamma = -1.6$ (dashed), and log $\Gamma = -1.2$ (dash-dot). The observed range for C II is indicated, and upper limits for C III, Si III, and Si IV are indicated with a downward arrow. (b) Same as (a), but with an attenuated AGN-source metagalactic spectrum from Giroux and Shapiro (1990).

For the normal galaxy-type spectrum of Bregman and Harrington (1986), the data are all well matched for $v_0 \sim 100$ km s^{-1}, $\Gamma_{BH} \sim 10^{-1.8}$ and metal abundances which are $10^{-2.5}$ times the solar values. For the AGN-source metagalactic spectrum of Giroux and Shapiro (1990), on the other hand, the data are matched with $v_0 \sim 100$ km s^{-1}, $\Gamma_{GS} \sim 10^{-2.2}$, and metal abundances which are 10^{-2} times solar. These flux levels are significantly higher than that of the radiation emitted by the flow, itself. Hence, unlike the case of our own galactic halo gas, self-ionization of the fountain flow is not sufficient to account for the observed quasar absorption lines. Finally, we note that isobarically cooling gas with Γ even as large as 10^{-1} cannot match the observations.

3. LARGE-SCALE EXPLOSIONS AND SUPERBUBBLES IN THE GALACTIC DISK AND HALO: MHD SIMULATIONS AND ANALYTICAL APPROXIMATIONS

The evolution of the interstellar superbubbles arising from sequential supernova explosions or winds from OB associations in the galactic disk were studied numerically, using a two-dimensional magneto-hydrodynamics (MHD) code (Mineshige, Shibata, and Shapiro 1990). We find that in the presence of horizontal magnetic fields of strength comparable to that in the galactic disk, $B = 3\ \mu G$, the vertical expansion of the superbubbles (the contact surface) can, under some conditions, be significantly inhibited by the effect of a decelerating $J \times B$ force, while, at the same time, the outermost effect of the disturbance actually propagates somewhat faster than in nonmagnetic cases, as an MHD shock or nonlinear wave. The conditions under which magnetic fields are dynamically important in the evolution of superbubbles have been discussed analytically, as well (Shapiro, Mineshige, and Shibata 1990). We have derived a new, analytical Kompaneets approximation for a two-dimensional, axisymmetric, steadily driven explosion in a nonmagnetic, exponential disk which we apply to this question.

3.1 Numerical Results

As an illustration, we show here results of a 2D, MHD, numerical simulation of a superbubble resulting from sequential supernovae. Our simulation in the (x,z) plane assumes a field $B = (3\mu G)\hat{x}$ (i.e. horizontal to the plane), a mass and energy input per explosion equivalent to 10 $M_\odot$ and 10^{51} erg deposited every 3×10^5 yr uniformly in a cylinder along the y-axis of radius 20 pc and length 500 pc, in an ambient medium at 10^4 K with density 1 cm^{-3} in the disk, which extends to height $z = 100$ pc, with a halo of density 10^{-2} cm^{-3} for $z > 100$ pc. Figures 3(a)-(c) show three time-slices for each of two simulations, one with and one without magnetic field, at roughly the same epoch. Figure 4 shows the qualitative features of the magnetized case. Our results are consistent with those described by Tomisaka elsewhere in this volume.

3.2 The Modified Kompaneets Approximation

When are magnetic fields dynamically important in the evolution of superbubbles? In order to help answer this, we have derived a new, analytical Kompaneets approximation for a steadily-driven explosion in a nonmagnetized, plane-stratified, exponential atmosphere with undisturbed ambient density $\rho \propto \exp(-z/H)$. According to this solution, the condition for "blow-out" to occur in the absence of magnetic field is given by:

$$L_{38} p_{-12}^{-3/2} \rho_{-24}^{1/2} H_2^{-2} \gtrsim (0.23, 0.34, 0.25, 0.38) \text{ for (AO, AS, IO, IS)}, \qquad (3.2.1)$$

https://doi.org/10.1017/S0074180900089373 Published online by Cambridge University Press

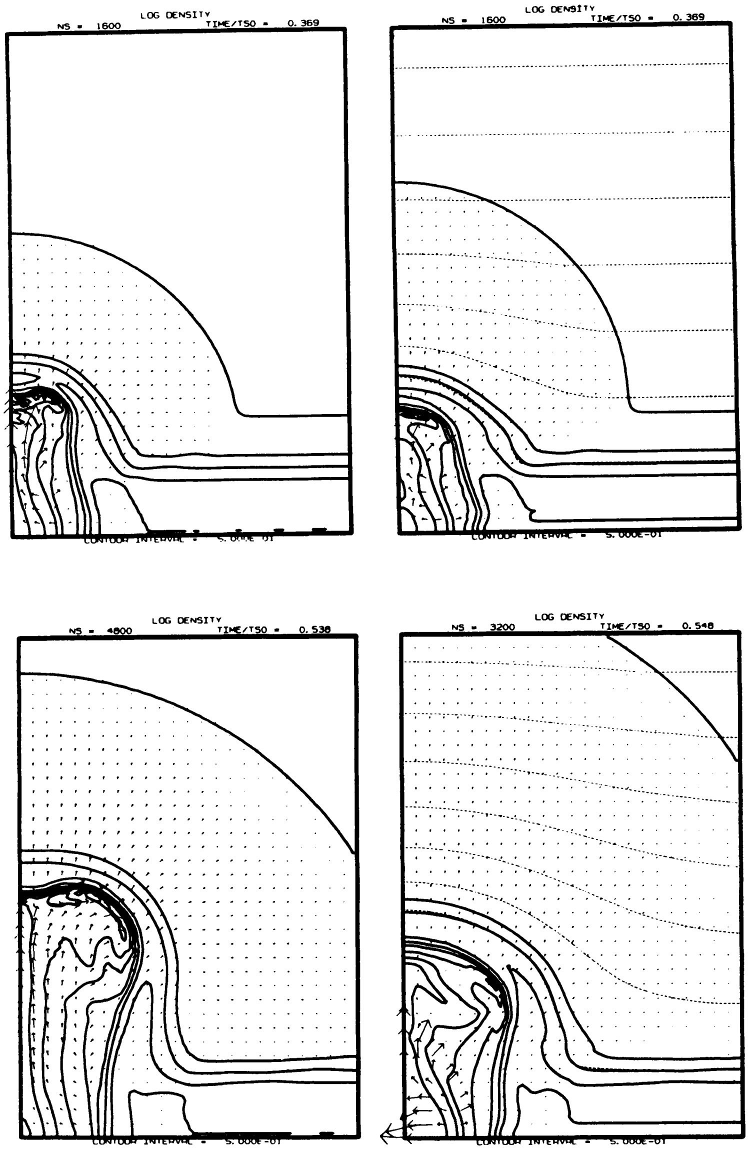

Figure 3. (a) (top) and (b) (bottom). Superbubble from sequential SN in disk-halo, with and without magnetic field. Left (B = 0). Right (B = 3μG). Density contour (thick lines) are logarithmically spaced by 0.5 dex from $\rho = 10^{-27} - 10^{-24}$ g cm^{-3}. Velocity vectors (arrows) and magnetic field lines (dashed lines) are also shown. Elapsed times in Myr = 10^6 yr are (a) 3.0 and (b) 4.4.

https://doi.org/10.1017/S0074180900089373 Published online by Cambridge University Press

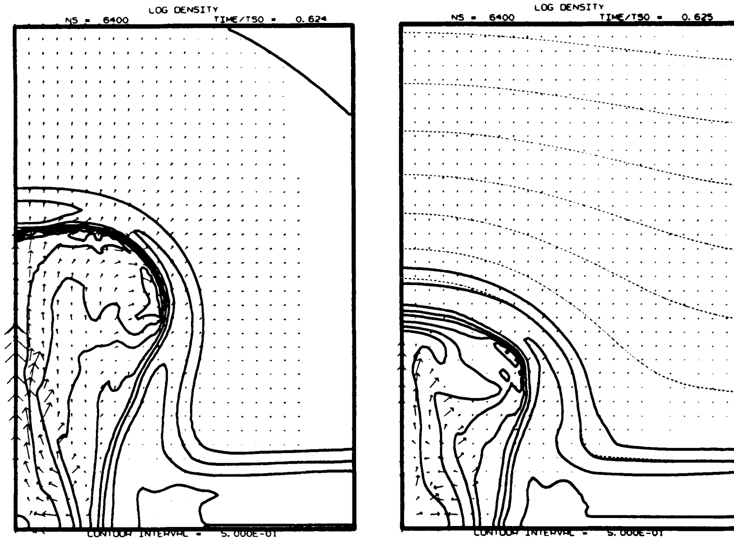

Figure 3. (c) Same as Figures 3(a), (b) except elapsed time is 5.1 Myr.

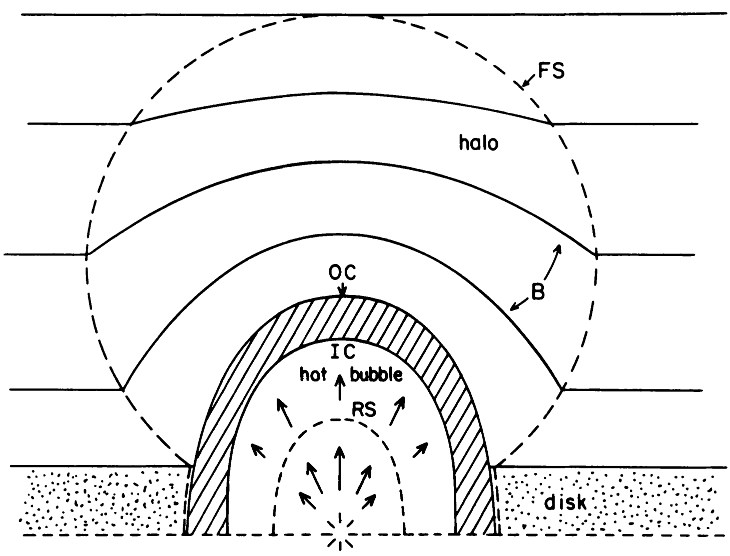

Figure 4. Schematic diagram of magnetic superbubble. Outer contact discontinuity ("OC"), inner contact discontinuity ("IC"), reverse shock ("RS"), and forward shock ("FS") are labeled.

where the central explosion energy injection rate at z = 0 has the constant luminosity $L_{38} \equiv L/(10^{38}\mathrm{erg\ s^{-1}})$, the ambient undisturbed gas pressure at z = 0 is $p_{-12} = p(z{=}0)/(10^{-12}\mathrm{erg\ cm^{-3}})$, $\rho_{-24} = \rho(z{=}0)/(10^{-24}\ \mathrm{g\ cm^{-3}})$, and $H_2 = H/(100\ \mathrm{pc})$, "AO" = adiabatic shock, one-sided case [$\rho \propto \exp(-z/H)$], "AS" = adiabatic shock, symmetric case [$\rho \propto \exp(-|z|/H)$], "IO" = isothermal shock, one-sided, and "IS" = isothermal shock, symmetric. This analytical expression is roughly consistent with the approximate numerical solutions of Mac Low and McCray (1988).

In order for a magnetic field to influence this explosion, it must be roughly true that the original magnetic energy in the volume swept up by the explosion exceeds the explosion energy. Suppose the undisturbed gas has $\beta = \beta_o = p_{gas}/p_{mag}$ = constant, independent of z, and condition (3.2.1) is already met. In that case, we find that magnetic fields are dynamically important and might inhibit "blow-out" if the following condition is met:

$$\beta_o \lesssim (2.0,2.1,2.1,2.3) \times \left[L_{38} p_{-12}^{-3/2} \rho_{-24}^{1/2} H_2^{-2}\right]^{-1} \text{ for (AO,AS,IO,IS).} \qquad (3.2.2)$$

4. MHD SIMULATION OF HALO CLOUD FORMATION BY THERMAL INSTABILITY

The nonlinear evolution of thermal instability in a density perturbation was studied as a model for the formation of clouds in the galactic halo (Mineshige, Shibata, Shapiro, and Tajima 1990). We have followed the evolution of a cloud analytically, using the isobaric approximation. The temperature of the cloud decreases explosively and reaches the minimum value in a time shorter than the initial cooling time scale. These features are confirmed by two-dimensional numerical simulations for nonmagnetic cases: the cloud formation takes place symmetrically in space and explosively in time. We have further included magnetic fields and gravity in our simulations. In contrast to the nonmagnetic cases, the shape of a cloud is vertically elongated by the presence of horizontal magnetic fields because the ambient gas cannot accrete onto the cloud across the field lines. In the case of strong magnetic fields with the initial ratio of the gas pressure to the magnetic pressure $\beta = 1$, the cloud is nearly suspended by the horizontal magnetic fields.

4.1 Numerical Results

As an illustration, we show results from our 2D, MHD simulations (in the x, z-plane) for a cloud forming by thermal instability in an initially, slight over-dense region in a radiatively cooling gas which starts at 10^6 K in magneto-hydrostatic equilibrium at constant $\beta = p_{gas}/p_{mag}$ in a uniform Galactic gravitational field, with mean density 10^{-27} g cm^{-3} at height z = 0. Comparison in Figure 5 of the magnetized case ($\beta = 1$ and $B \| \hat{x}$) with the unmagnetized case shows that in the former, magnetic fields decelerate the vertical precipitation motion of the cloud perpendicular to B (notice the much smaller velocity vectors in the bottom time-slices for $\beta = 1$ compared to the top time-slices for B = 0).

5. THE GALACTIC DYNAMO IN THE PRESENCE OF A GALACTIC FOUNTAIN

The conventional picture of the galactic dynamo mechanism for the generation and maintenance of the large-scale magnetic field in disk galaxies (e.g. Parker 1971) neglects effects due to the presence of a gaseous halo and of the disk-halo interaction. Possible

https://doi.org/10.1017/S0074180900089373 Published online by Cambridge University Press

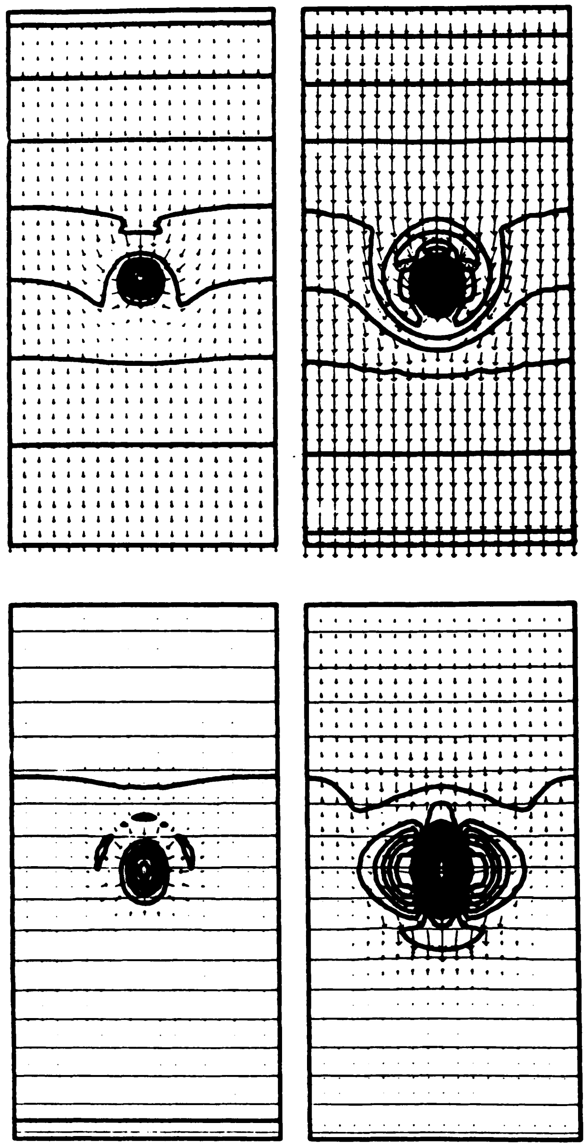

Figure 5. Time-slices of simulation, with (bottom panels) and without (top panels) magnetic field. Density contours are thick lines with logarithmic spacing of 0.5 dex in density, magnetic field lines are thin lines, velocity vectors are arrows. Times (in units of 10^8 yr) are 0.15 (left panels) and 0.298 (right panels).

such effects include buoyant and explosion-driven escape of magnetic flux from the disk into the halo, helicity associated with galactic fountain flows which circulate gas from the disk to the halo and back to the disk, velocity shear associated with a gradient in galactic rotation velocity in the direction perpendicular to the galactic plane, resistive diffusion of the field in the z-direction or the possibility that turbulent resistivity is, instead, confined to the disk and absent from the halo, and the presence of z-motions and of gradients in the z-direction in general.

The standard equation of $\alpha\omega$-dynamo theory is the modified induction equation

$$\frac{\partial \mathbf{B}}{\partial t} = \nabla \times (\mathbf{V} \times \mathbf{B}) + \eta \nabla^2 \mathbf{B} + \nabla \times (\alpha \mathbf{B}), \tag{5.1}$$

where $\mathbf{B}$ = magnetic field, $\mathbf{V}$ = fluid velocity, both averaged locally over space, η = turbulent resistivity and α represents the effect of helical turbulence, or cyclonic convection. This helical convection is characterized by the occurrence of vertical flows in a differentially rotating gaseous disk which diverge (expand) or converge (compress) for upward or downward motion, respectively, as expected if the disk gas density decreases with distance from the central plane. As estimated by Vainshtein and Ruzmaikin (1972), for example, this leads to an α-effect of strength $\alpha \approx \ell^2\omega/H$, where ℓ is the length scale of an individual turbulent eddy, H is the disk vertical density scale height, and ω is the angular rotation velocity of the disk. For the conventional picture of the galactic dynamo confined to the galactic disk, $\ell_{disk} \sim H_{disk} \sim 100$ pc are assumed.

Galactic fountain/superbubble flows, however, provide even larger-scale, cyclonic convection suitable for generating its own α-effect. We estimate that such flows can produce a "galactic fountain" α-effect characterized by $\alpha_{GF} \approx \ell^2_{GF}\omega/H_{GF}$, where $\ell_{GF} \gtrsim 1$ kpc (e.g. ℓ_{GF} is at least as large as the size of a superbubble that breaks out of the disk) and $H_{GF} \gtrsim$ kpc's (e.g. H_{GF} ranges from the size of a superbubble at break-out to the density scale-height of the galactic halo gas). Hence, $\alpha_{GF}/\alpha_{disk} \sim (\ell_{GF}/\ell_{disk})(\ell_{GF}/H_{GF}) \sim 10$ is possible. Apparently, a galactic-fountain-dominated galactic dynamo may contribute significantly to the origin and evolution of the large-scale magnetic fields in galaxies.

ACKNOWLEDGEMENTS

I am grateful to Robert Benjamin, Shin Mineshige, Kazunari Shibata, Toshiki Tajima, and Robert Bishop for their collaboration in the research which I have previewed here. Robert Benjamin and I are grateful to John Raymond for making his hot gas atomic parameter data set available to us. We also thank Mark Giroux for his advice and assistance. This work was supported in part by Robert A. Welch Foundation Grant No. F-1115, Texas Advanced Research Program Grant No. 4132, NASA Training Grant No. NGT-50519, and an Alfred P. Sloan Foundation Fellowship in Physics. All of our numerical calculations were performed on the University of Texas Center for High Performance Computing Cray X/MP.

REFERENCES

Allen, C. W. (1973) *Astrophysical Quantities* (London: The Athlone Press).
Bregman, J. N., Harrington, J. P. (1986) *Ap. J.*, **309**, 833.
Edgar, R. J., Chevalier, R. A. (1986) *Ap. J. (Lett.)*, **310**, L27.

Giroux, M. L., Shapiro, P. R. (1990) in *Physical Processes in Fragmentation and Star Formation*, eds. R. Capuzzo-Dolcetta, C. Chiosi, and A. De Fazio (Boston: Kluwer Academic), 71.
Kutyrev, A. S., Reynolds, R. J. (1989) *Ap. J. (Lett.)*, **344**, L9.
Mac Low, M-M., McCray, R. (1988) *Ap. J.*, **324**, 776.
Martin, C., Bowyer, S. (1990) *Ap. J.*, **350**, 242.
Mineshige, S., Shibata, K., Shapiro, P. R. (1990) *Ap. J.*, submitted.
Mineshige, S., Shibata, K., Shapiro, P. R., Tajima, T. (1990) in preparation.
Parker, E. N. (1971) *Ap. J.*, **163**, 255.
Raymond, J. C. (1987) private communcation.
Raymond, J. C., Smith, B. W. (1977) *Ap. J. Suppl.*, **35**, 419.
Sargent, W.L.W., Steidel, C. C., Boksenberg, A. (1990) *Ap. J.*, **351**, 364.
Savage, B. D. (1988) in *QSO Absorption Lines: Probing the Universe*, eds. J. C. Blades, D. Turnshek, C. A. Norman (New York: Cambridge U. Press), 195.
Savage, B. D., Massa, D. (1987) *Ap. J.*, **314**, 380.
Shapiro, P. R., Benjamin, R. A. (1990) in preparation.
Shapiro, P. R., Field, G. B. (1976) *Ap. J.*, **205**, 762.
Shapiro, P. R., Mineshige, S., Shibata, K. (1990) *Ap. J.*, submitted.
Songaila, A., Bryant, W., Cowie, L. L. (1989) *Ap. J. (Lett.)*, **345**, L71.
Spitzer, L. (1990) *Ann. Rev. Astron. Astrophys.*, **28**, in press.
Vainshtein, S. I., Ruzmaikin, A. A. (1972) *Sov. Astr.*, **15**, 714.